Apparent Pressures on Multi-Propped Retaining Walls in Soils Under Drained Conditions with Shallow Water Table

L. Andrade Viana, N.M. da Costa Guerra

Abstract. In the design of flexible retaining walls supported by several levels of struts, apparent design diagrams are frequently used, particularly to predict the loads on the struts. In the case of sandy soils, the traditional design diagrams do not consider water table. The present work deals with apparent design diagrams for cases considering water table. A brief analysis of the problem based on published information is presented. Stress-strain finite element analyses are applied to a case study, comparing situations without water table with others where the water table is assumed. For the cases where water table is assumed two types of conditions are considered: those where seepage is allowed and those where it is not. A parametric analysis is performed to study the effects on soil pressures and on apparent pressures of geometrical and mechanical parameters of the soil and structure. From the analysis of the results a proposal for the apparent diagrams for the design of retaining walls performed in soils under drained conditions with water table above the bottom of the excavation is presented.

Keywords: multi-propped retaining walls, apparent earth pressures, water pressures, seepage.

1. Introduction

Numerical methods are commonly used in the design of multi-propped retaining walls. They allow the stress-strain step-by-step analysis of the construction procedure and therefore the prediction of the displacements induced in the supported soil, the forces and bending moments on the wall and the loads on the struts. However, its use needs the pre-definition of several geometrical and structural characteristics. In the case of the wall and struts, such pre-definition needs the prediction of the loads installed, which is frequently done using apparent design diagrams.

The most known and used apparent design diagrams are those proposed by Terzaghi & Peck (1967). In case of sandy soils, the diagram is rectangular, with horizontal stress given by:

$$\sigma_H = 0.65 K_a \gamma H \quad (1)$$

in which K_a is the Rankine active earth pressure coefficient, γ is the unit weight of the soil and H is the depth of the excavation.

These diagrams were the result of monitoring the loads on the struts of several multi-propped flexible retaining walls throughout a few decades of the twentieth century. In most cases, for drained situations, the adopted construction procedure allowed lowering the water table in cases where it was above the bottom of the excavation and therefore no water pressures existed on the retaining walls.

There is no generally accepted way to take into account in the apparent diagrams the existence of water table above the bottom of the excavation in flexible retaining walls supported by several levels of struts. When the excavation is carried out below the water table, without lowering it, and the wall is impermeable, a substantial part of pressures on the wall will be due to water. When seepage is not allowed (because the wall was extended to an impermeable stratum) the structure has to be designed to withstand the hydrostatic pressures. Strom & Ebeling (2001) proposed an apparent diagram considering both soil and water pressures (see Fig. 1).

This diagram is based on Terzaghi and Peck's, using an average effective unit weight to which the pore-water pressure is added. The average effective unit weight, γ_e, can be calculated by either of two methods, in which the soil above the water table is considered with the moist unit weight, γ, and the soil below the water table is considered with the buoyant unit weight, γ'.

In method 1 (Strom & Ebeling, 2001), γ_e is the weighted average using depths H - z_w and z_w shown in Fig. 2:

$$\gamma_e = \frac{\gamma'(H - z_w) + \gamma z_w}{H} \quad (2)$$

In method 2 (Ebeling & Morrison, 1992), γ_e is the weighted average using A_1 and A_2 also shown in Fig. 2:

$$\gamma_e = \frac{\gamma' A_1 + \gamma A_2}{A_1 + A_2} = \frac{\gamma'(H - z_w)^2 + \gamma z_w^2}{H^2} \quad (3)$$

In the particular case of water table on the ground surface the application of methods 1 and 2 results in the same

Laís Andrade Viana, MSc, Departamento de Engenharia Civil, Faculdade de Ciências e Tecnologia, Universidade Nova de Lisboa, Lisboa, Portugal. e-mail: l.viana@campus.fct.unl.pt.
Nuno M. da Costa Guerra, Associate Professor, UNIC, Departamento de Engenharia Civil, Faculdade de Ciências e Tecnologia, Universidade Nova de Lisboa, Lisboa, Portugal. e-mail: nguerra@fct.unl.pt.
Submitted on July 16, 2015; Final Acceptance on November 2, 2015; Discussion open until April 30, 2016.

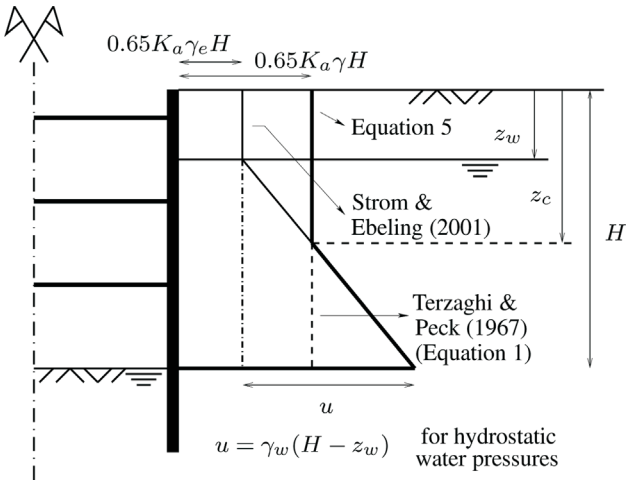

Figure 1 - Apparent diagrams for sandy soils for no water table (Terzaghi & Peck, 1967) and for water table above the bottom of the excavation (Strom & Ebeling, 2001) and proposed correction of this method, given by Eq. 5.

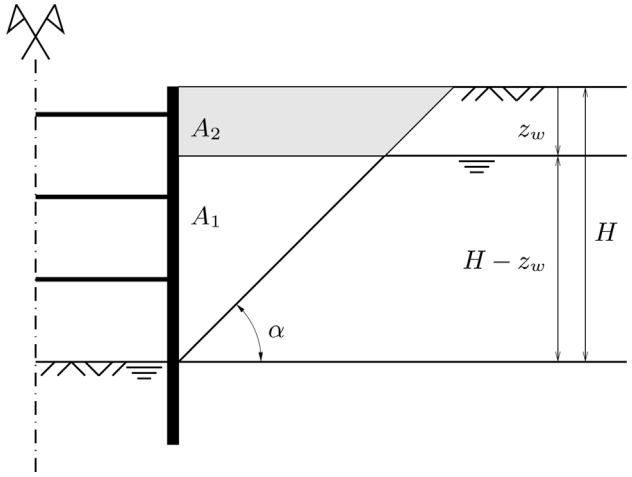

Figure 2 - Geometric parameters for determining the effective unit weight for partially submerged soils. Angle α is the angle defining the failure wedge.

solution and the average effective unit weight is equal to the buoyant unit weight.

The resulting diagram implies the consideration up to a certain depth, z_c, given by:

$$z_c = 0.65K_a H\frac{\gamma - \gamma_e}{\gamma_w} + z_w \quad (4)$$

of a total pressure that is lower than the one that would be considered if there were no water table, which does not seem to make much sense. Therefore, a proposal that seeks to rectify this aspect is also shown in Fig. 1 and the horizontal pressures take the following values (see Andrade Viana, 2014):

$$\sigma_H = \begin{cases} 0.65K_a\gamma H & , \ z \le z_c \\ 0.65K_a\gamma_e H + \gamma_w(z - z_w), & z > z_c \end{cases} \quad (5)$$

In cases where seepage is allowed around the wall into the excavation, with steady-state seepage conditions, there are seepage forces on the ground. The diagrams, adapted from the previous, consider, instead of the buoyant unit weight γ′, this unit weight plus the seepage forces. In addition, the water pressures will no longer be hydrostatic and u (see Fig. 1) will therefore not be $\gamma_w(H - z_w)$ and the linear distribution will be a simplification. It is possible to verify that this proposal leads to lower total pressures on the wall when compared to the ones from the hydrostatic case, and therefore only the hydrostatic ones will be shown in the paper, for comparison with the results obtained from the numerical analyses.

The diagrams described above have not been confirmed either by monitoring or numerical analyses. Therefore, the present work intends to numerically obtain apparent diagrams, for cases considering the presence of the water table in the soil. It is somehow interesting that a numerical procedure is felt useful to obtain diagrams of the same type as others that were probably only developed because of the lack of such advanced techniques, at the time.

2. Modelling

Stress-strain finite element analyses were performed for this study, using the finite element program Plaxis (2014). The problem consists of a symmetrical excavation supported by a multi-propped retaining wall and plane strain conditions are assumed.

Five scenarios were analyzed and they are schematically shown in Fig. 3:

- Scenario A: no water table, the wall does not reach the rigid impermeable stratum.
- Scenario B: water table at depth z_w; the wall does not reach the rigid impermeable stratum and the water level is lowered inside the excavation by continuous pumping. Seepage modelling is performed.
- Scenario C: no water table, the wall reaches the rigid impermeable stratum and it can not rotate at the toe.
- Scenario D: water table at depth z_w; the wall reaches the rigid impermeable stratum and it can not rotate at the toe. No seepage is allowed.
- Scenario E: water table at depth z_w; the wall reaches an almost impermeable stratum and the water level is lowered inside the excavation by continuous pumping. Seepage modelling is performed, even though seepage occurs mainly in the stratum with very low permeability.

The excavation was modelled in alternating stages of excavation and installation of strut levels. The excavation stages also consider that the water level is lowered inside the excavation (scenarios B, D and E) and the calculation of the associated seepage (scenarios B and E). It should also be mentioned that the soil was assumed homogeneous and

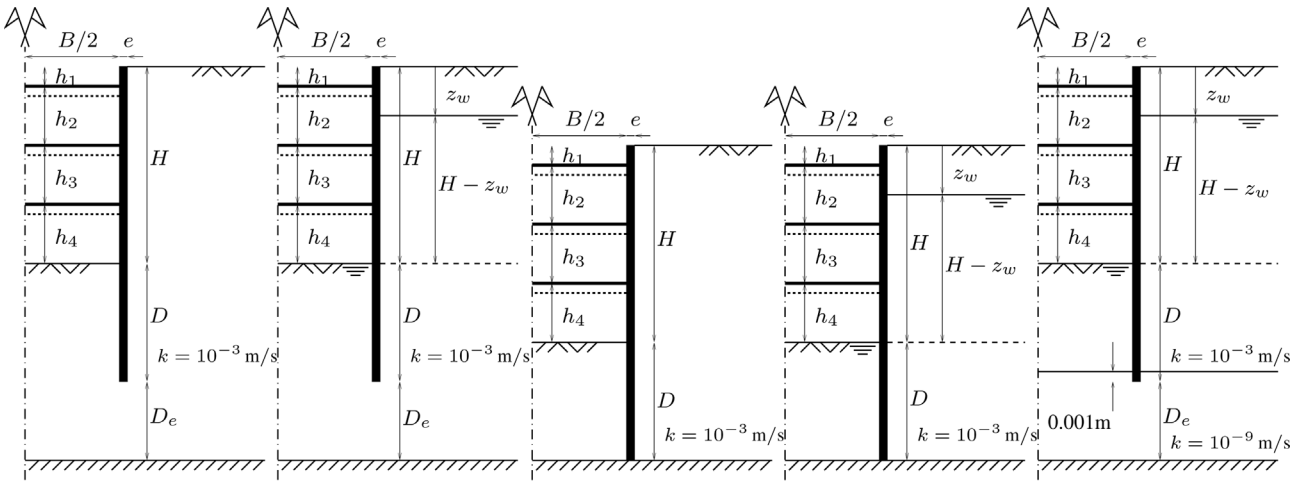

Figure 3 - Schematic representation of scenarios A, B, C, D and E.

isotropic. If real conditions of the soil involved heterogeneity and (or) anisotropy, the groundwater flow could have a significant effect on the pressures on the wall (Kaiser & Hewitt, 1982).

The wall and the struts were admitted linear elastic. The soil was modelled by the "Hardening Soil Model" (Schanz *et al.*, 1999). The HSM is an elastoplastic type of hyperbolic model, formulated in the framework of shear hardening plasticity. The model also involves compression hardening to simulate irreversible compaction of soil under primary compression (Plaxis, 2014).

Limiting states of stress are described by means of the shear strength angle, ϕ', the effective cohesion, c', and the dilatancy angle, ψ. Soil stiffness is described by using three different input stiffnesses: the secant triaxial loading stiffness to half of the tensile strength, E_{50}, the triaxial unloading and reloading stiffness, E_{ur}, and the oedometer loading stiffness, E_{oed}. These stiffnesses depend on stress-state according to the relations:

$$E_{50} = E_{50,ref}\left(\frac{\sigma'_3 + c'_{ref}\cot\phi'}{p'_{ref} + c'_{ref}\cot\phi'}\right)^m \quad (6)$$

$$E_{ur} = E_{ur,ref}\left(\frac{\sigma'_3 + c'_{ref}\cot\phi'}{p'_{ref} + c'_{ref}\cot\phi'}\right)^m \quad (7)$$

$$E_{oed} = E_{oed,ref}\left(\frac{\sigma'_1 + c'_{ref}\cot\phi'}{p'_{ref} + c'_{ref}\cot\phi'}\right)^m \quad (8)$$

in which m is a power that expresses the dependence of the soil stiffness with the stress state in the soil, p'_{ref} is a reference stress, usually taken equal to 100 kPa, σ'_1 is the major principal stress and σ'_3 is the minor principal stress. In order to characterize the soil stiffness the following reference stiffnesses are required: $E_{50,ref}$, $E_{ur,ref}$ and $E_{oed,ref}$. As average values for various soil types, $E_{ur,ref} = 3E_{50,ref}$ and $E_{oed,ref} = E_{50,ref}$ are suggested as default settings (Plaxis, 2014).

3. Case Study

The case study has the following values for the geometrical parameters: $B/2$ = 5 m; e = 0.4 m; H = 10 m; D = 6 m; D_e = 4 m; h_1 = 1 m; $h_2 = h_3 = h_4$ = 3 m; z_w = 0 m. The excavation was modelled in stages, for a total of nine stages. It was performed in four levels of excavations and the wall is supported by three levels of struts.

The soil was considered as a sandy soil with drained behaviour. In scenarios A and C the moist unit weight was set as 20 kN/m^3. In scenarios B, D and E the water table was considered on the ground surface and the saturated unit weight was also taken equal to 20 kN/m^3.

The chosen stiffness parameters intend to portray the behaviour of a medium sand: $E_{50,ref}$ = 25000 kPa, $E_{ur,ref}$ = 75000 kPa, $E_{oed,ref}$ = 25000 kPa and m = 0.5. It was assumed a shear strength angle, ϕ', of 30°, a reference effective cohesion, c'_{ref}, of 1 kPa and a dilatancy angle, ψ, of 1°. The at rest earth pressure coefficient, K_0, was taken equal to 0.5. The soil was considered with homogeneous hydraulic characteristics (permeability coefficient in the horizontal direction equal to the permeability coefficient in the vertical direction, $k_x = k_y$). This coefficient was taken equal to 10^{-3} m/s. In scenario E the soil below the wall was considered with a very low permeability coefficient, in both directions, of 10^{-9} m/s. All other parameters were considered equal to the ones of the soil above.

Interfaces were modelled by joint elements and its strength and stiffness properties are defined by the strength reduction factor, R_{inter} (Plaxis, 2014), which was set as 0.67.

The wall was considered built before the excavation, with elastic characteristics of a reinforced concrete wall with a bending stiffness, EI, of 160000 kNm^2/m. Given that

it is an ”infinite” wall, since the analysis is in plane strain conditions, a null Poisson’s ratio, ν, was adopted.

The wall weight per unit area was considered equal to 10 kN/m/m.

The stiffness of the struts was chosen by performing preliminary calculations using scenarios A and C, so that pressures on the wall and apparent pressures inferred from the maximum loads on the struts roughly correspond to the apparent diagrams of Terzaghi and Peck with horizontal stresses given by Eq. 1. The same characteristics were adopted in scenarios B, D and E. Thus, the struts were assumed as linear elastic with axial stiffness, *EA*, of 120000 kN/m.

Figure 4 shows the distribution of hydraulic head in the soil mass after the last excavation stage in scenarios B and E. The distributions of hydraulic head correspond to the expected and it is possible to note that the lines defined by color changes correspond to equipotential lines.

Figure 5 shows the displacements obtained for the wall and for the surface of the supported soil mass after the last stage of excavation. It can be observed that the displacement values corresponding to scenarios with water (B, D and E) are substantially higher than those associated to scenarios without water (A and C). In particular, in scenario B, wherein the wall is not based on rigid impermeable stratum and seepage is allowed, the displacements of the wall and, thus, of the surface of the supported soil, are particularly high. It is interesting to notice that the displacements for this scenario (B) are greater than the ones for scenario E, where the wall toe can move and water pressures on the right side are hydrostatic and larger than in scenario B.

Figure 6 shows the plastic points obtained after the last excavation stage for all scenarios that were analised. It is possible to observe that in scenarios A and C there are few failure points which occur specially in the soil-structure interface. In scenario B failure points occur mainly in the soil mass, showing the beginning of a sliding surface; it should be noted that this occurs even though the global safety factor against the hydraulic uplift is, in this case, relatively high (FS = 1.43). In scenario D failure points occur especially in the soil-structure interface and in a band of soil inside the excavation, without any hint of a sliding surface. In scenario E there is, again, an intermediate situation between scenarios B and D, with failure points in soil-structure interface and also the beginning of a potential sliding surface in the soil on the right side of the wall.

Figure 7 shows the results obtained after the last stage of excavation for total, effective and pore water pressures on the wall. It also shows the apparent pressures inferred from the maximum loads on the struts. The apparent diagram of Terzaghi and Peck (Eq. 1) and the apparent diagram given by Eq. 5 are also shown in Figs. 7(a) and 7(b), for comparison with the results obtained.

Scenarios A and C have equal total and effective pressures as there are no pore water pressures. In scenario B pore water pressures deviate progressively from hydrostatic pressures, while in scenarios D and E they are equal to hydrostatic pressures. In fact, in scenario E, the seepage is negligible and therefore the pore water pressures are very similar to hydrostatic pressures.

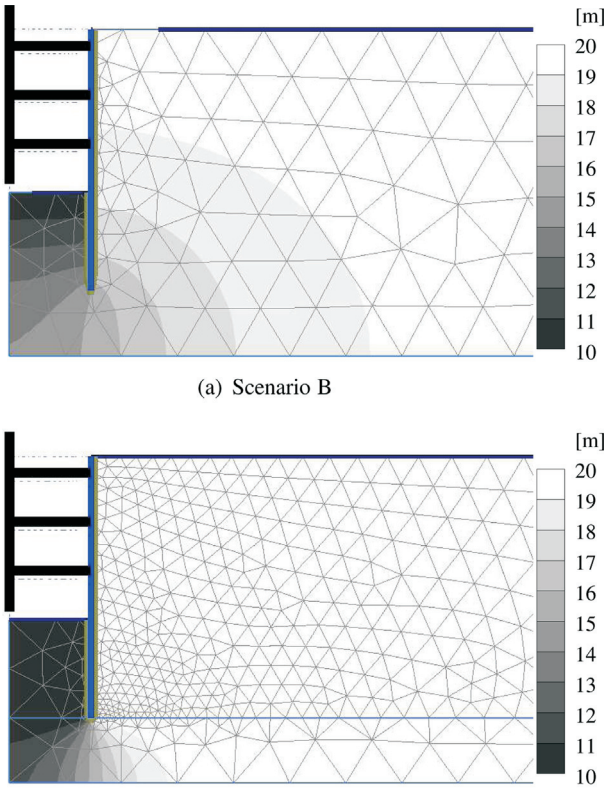

Figure 4 - Distribution of water head after the last excavation stage.

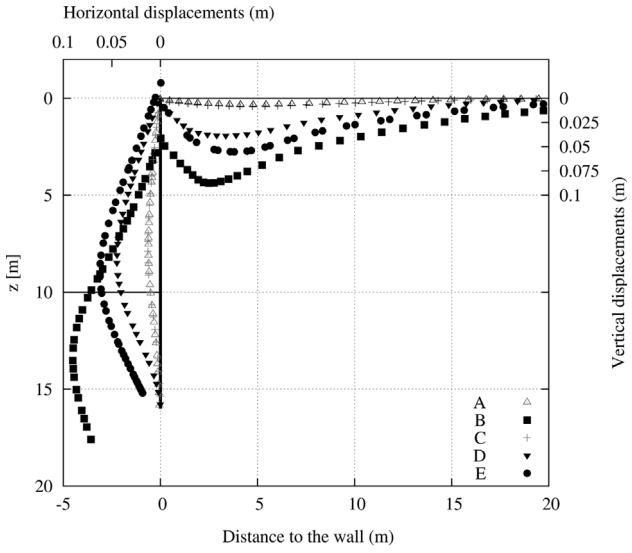

Figure 5 - Displacements of the wall and of the surface of the supported soil mass after the last excavation stage.

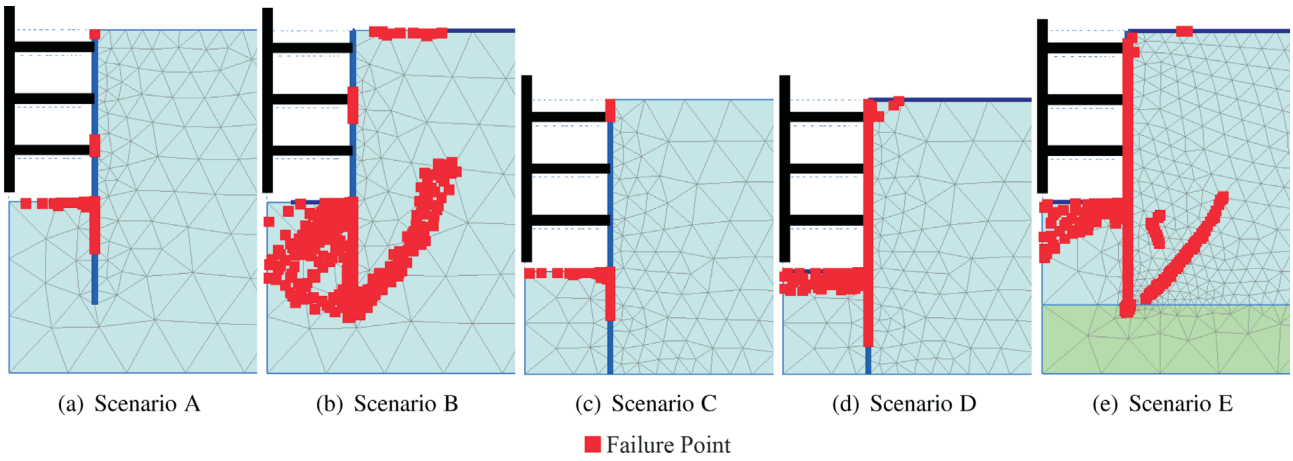

Figure 6 - Failure points after the last excavation stage.

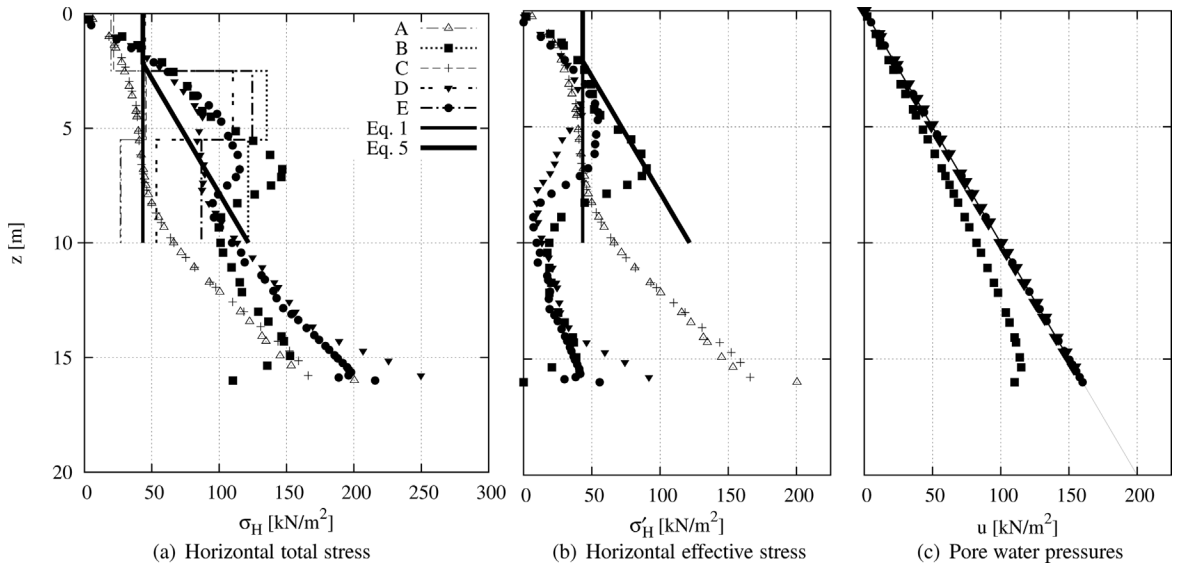

Figure 7 - Pressures on the flexible retaining wall after the last excavation stage (symbols) and apparent pressures inferred from the maximum loads on the struts (lines; Fig. 7(a)).

In scenarios A and C the distribution of total stresses on the wall approaches the apparent diagrams of Terzaghi and Peck. Indeed, as referred, the axial stiffness adopted for struts was chosen so that the distribution of pressures on the wall for these scenarios would be approximately constant in depth and equal to the value obtained from Eq. 1.

In scenario B total stresses on the wall are greater than those corresponding to the apparent diagram given by Eq. 5. This diagram is, up to a certain depth, similar to the obtained distribution of effective stresses, despite this apparent diagram being established in terms of total stresses. It can be seen that the apparent pressures corresponding to the last level of struts are very close to the ones corresponding to the second level of struts. In fact, the apparent pressures corresponding to the last level of struts are, up to a certain depth, lower than the distribution of total stresses on the wall at the same depth, while, from that same depth, the apparent pressures become greater than the distribution of total stresses on the wall.

In scenario D total stresses on the wall are also greater than the apparent diagram given by Eq. 5. However, it can be noted that in this scenario the distribution of total stresses on the wall is closer to this apparent diagram than in scenario B. Thus, contrary to what is verified in the situation in which the existence of water level is not considered, the existence of a rigid impermeable stratum shows considerable influence on the distribution of total pressures on the wall. It can be seen that in this scenario the apparent pressures corresponding to the last level of struts are much lower than the distribution of total stresses on the wall at the same depth. This is probably due to the fact that the wall is embedded in a more competent stra-

tum, which is responsible to absorb a significant percentage of the pressures.

In scenario E there is an intermediate situation between scenarios B and D, with total stresses on the wall that remain greater than the apparent diagram given by Eq. 5. It is interesting to note that, when compared with scenario D, in scenario E the apparent pressures corresponding to the last level of struts are much closer to the distribution of total stresses on the wall. It is also interesting to notice that effective stresses are greater at the upper part of the wall and much lower at the bottom than in cases where soil is considered dry.

Figure 7 shows that the diagrams proposed in the literature are not suitable approximations for the distribution of pressures on the wall or the apparent pressures for the cases where water table was considered. Therefore, this justifies further research and, in particular, the parametric analysis presented below.

4. Parametric Analysis

4.1. Cases

Based on the case study, parametric analyses of several geometrical and mechanical aspects were performed. A brief overview of all the analyses performed is presented in Table 1.

Those analyses were performed in two stages. In the first stage (left part of Table 1) the parametric analyses consisted in the variation of one parameter at a time. In these analyses scenarios A, B, C and D were studied. For example, when the analysis of the variation of the embedded length of the wall was performed, only this parameter took different values: the one corresponding to the case study itself (in bold in the Table 1), a value above and another below it. A similar procedure was performed for the axial stiffness of the struts, the wall bending stiffness, the width of the excavation, the scale of the problem and the unit weight of the soil. In the parametric analysis of the scale of the problem, two additional calculations were performed:

Table 1 - Cases analysed in the parametric analyses.

Case	A	B	C	D	B	D	E
D [m]	3/**6**/8		2/**6**/8		3/**6**/8	2/**6**/8	
EA [kN/m]	0.2 EA_{cs} / $\boldsymbol{EA}_{cs}$ / 5EA_{cs}				$\boldsymbol{EA}_{cs}$		
EI [kNm^2/m]	EI_{cs} /8 / $\boldsymbol{EI}_{cs}$ / 8EI_{cs}				$\boldsymbol{EI}_{cs}$		
B [m]	6/**10**/20				**10**		
Scale	×0.5 / ×**1** / ×2				×**1**		
Soil - S	**1**/2				**1**/2		
γ [kN/m^3]	17.5/**20**/25				**20**		
z_w [m]	–	**0**	–	**0**	**0**/2.5/5/7.5/10		

$\boldsymbol{EA}_{cs}$ and $\boldsymbol{EI}_{cs}$ are the values adopted in the case study.

one where all dimensions of the problem were halved and one other where they were doubled. For the analysis of the variation of the mechanical characteristics of the soil, only two soils were studied: the soil that was considered in the case study (soil 1, in bold in the Table 1), and a soil with better mechanical characteristics (soil 2): $\phi' = 40°$, $\psi = 8°$, $E_{50,ref}$ = 90000 kPa, $E_{ur,ref}$ = 270000 kPa and $E_{oed,ref}$ = 90000 kPa. For soil 2, the at rest earth pressure coefficient was taken equal to 0.8, assuming an overconsolidated material.

In the second stage of the parametric analyses (right part of Table1), different depths of the water table, z_w, and different embedded lengths of the wall, for both soils – 1 and 2 – were considered. In these analyses scenarios B, D and E were studied.

As previously presented, the main objective of this paper is to propose apparent diagrams that can be used in the design of flexible retaining walls with water table above the bottom of the excavation. For such purpose, an overall analysis of all calculations is needed. The procedure followed is next presented as an example, and the same steps were taken for all the other analyses.

4.2. Example: analysis of the variation of the embedded length of the wall, *D*

As an example of the adopted procedure, the analysis of the variation of the embedded length of the wall is presented for all scenarios A to E. The pressures on the flexible retaining wall after the last excavation stage and apparent pressures inferred from the maximum loads on the struts are, for these cases, shown in Fig. 8.

In scenarios A and C the total stress distributions on the wall do not show major differences between the results obtained for each adopted value for the embedded length of the wall. However, for very small values of D, in scenario C it is possible to observe a change of the pressure distributions that show greater values for lower values of length D for greater depths and the reverse more superficially. In scenario B the distribution of total stress on the wall does not have a continuous evolution. Also, for D = 8 m, apparent pressures are lower than the ones for D = 6 m; however, for D = 3 m, apparent pressures at the lowest level significantly increase. This is due to the fact that in this case, the hydraulic uplift safety factor is very low. Also, it can be seen that for the lowest value of D, apparent pressures inferred from the strut loads are very large for scenario B. It should however be noticed that these correspond to unusual situations with very low hydraulic uplift safety factors. In scenario D, in the middle of the excavation height, the greater the embedded length of the wall, the greater the stress. In the last meters of the excavation height there is an inversion of this relationship. The apparent pressures show greater difference between the results corresponding to each embedded length of the wall the greater the depth. In scenario E the pressure distributions do not show major dif-

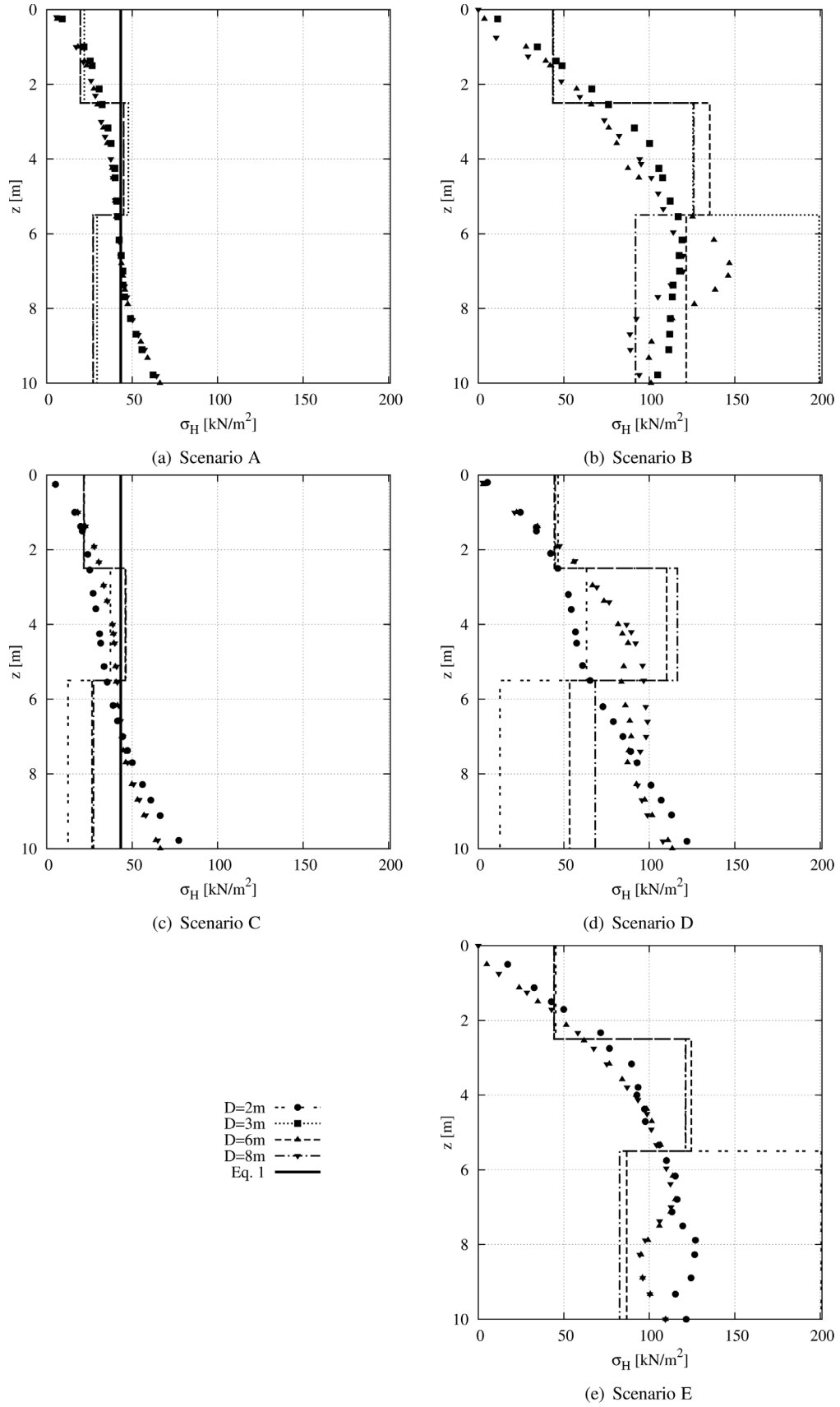

Figure 8 - Analysis of the variation of the embedded length of the wall: pressures on the flexible retaining wall after the last excavation stage (symbols) and apparent pressures inferred from the maximum loads on the struts (lines).

ferences between the results obtained for each adopted value for the embedded length of the wall, except, however, for the results corresponding to the embedded length of the wall with very small value (2 m). It is possible to note that in this case the pressures are globally higher than those corresponding to other cases. In this case this is caused by the large water pressures on one side of the wall and the considerably lower ones at the other side.

The results obtained after the last excavation stage for the pressures on the wall and for the apparent pressures (inferred from the maximum loads on the struts) were converted into dimensionless quantities by determining the ratio between the obtained pressures and the ones from Terzaghi and Peck's diagram (without water table):

$$\beta = \frac{\sigma_H}{0.65 K_a \gamma H} \quad (9)$$

and are shown in Fig. 9. This figure includes a proposed diagram that will be presented in section 5.

Figure 9 shows that the results can be reasonably normalized using Eq. 9, resulting in values of β approximately constant for each set of calculations. The same representation will be used for the other results obtained in the parametric analysis.

4.3. Analysis of the variation of other geometric and mechanical aspects

The same procedure followed in subsection 4.2 was adopted for the different parameters shown in Table 1 and the results for the dimensionless pressures are shown in Appendix A in Figs. A.1 to A.4. Scenarios B and D are the subject of the analysis; however, scenarios A and C are also studied for comparison.

It can be briefly mentioned that in the case where high water table with steady-state seepage is considered (Scenario B), the parameters that show greater influence on pressures on the retaining wall and on apparent pressures using the loads on the struts are: embedded length of the wall, width of excavation, mechanical characteristics of the soil and unit weight of the soil (which is more relevant in Soil 1); the parameters that have less influence than the previous ones are: axial stiffness of the struts, bending stiffness of the wall and scale of the problem.

In the case where high water table with hydrostatic pressures is considered (Scenario D), the parameters that show greater influence on pressures on the retaining wall and on apparent pressures using the loads on the struts are: embedded length of the wall, bending stiffness of the wall (in contrast to what is verified for Scenario B), mechanical characteristics of the soil and unit weight of the soil (which, as for Scenario B, is more relevant in Soil 1); the parameters that have less influence than the previous ones are: axial stiffness of the struts, scale of the problem (which have greater influence on the apparent pressures using the loads on the struts), but mostly the width of excavation (which does not have great influence, the opposite of what is verified in Scenario B).

Results represented in the dimensionless way shown by Eq. 9, as performed in Figs. A.1 to A.4, show approximately constant values of β, which means that this is an adequate way of presenting the results. These figures, as in Fig. 9, include the same proposed diagram that will be presented in Section 5.

4.4. Analysis of the variation of the depth of the water table (z_w)

Parametric analyses to study the influence of the variation of the depth of the water table were also performed and the results of the dimensionless pressures in scenario B are shown in Fig. 10 as an example.

As expected, the more shallow the water table, the greater the pressures. The lower the z_w, the greater the difference between the distribution of total pressures on the wall and the apparent pressures inferred from the strut loads, specially at the depth corresponding to the last strut level. For $z_w/H = 1$ soil 1 leads to greater normalized pressure on the wall than the soil 2. However, for water table closer to the ground surface, there is a reversal of this relation.

Scenarios D and E were also studied in order to analyse the influence of the depth of the water table variation and the results of the dimensionless pressures are shown in Appendix B in Figs. B.1 and B.2, respectively. As expected, it can be seen that shallower water tables result in greater pressures on the wall and greater apparent pressures. As in previous figures, Figs. 10, B.1 and B.2 include proposed diagrams (now depending on the water table depth) that will be presented next.

5. Proposal for Apparent Pressures

For cases without water table, scenarios A and C (Figs. A.1 and A.3), the dimensionless horizontal stresses, β, are reasonably approximated by 1.00, corresponding to the diagram of Terzaghi & Peck (1967) (Eq. 1). Moreover, this value remained globally adequate in most of the analyses (see Figs. 9(a), 9(c), 10(a), A.1, A.3, B.1(a) and B.2(a)), showing the suitability of the traditional diagram of Terzaghi and Peck as a conservative diagram for the results of the pressures.

For cases where water table is taken into account, scenarios B, D and E, the results obtained for the total pressures on the wall and apparent pressures inferred from maximum loads on the struts allow to propose apparent diagrams. These diagrams are also shown in Figs. 9, 10, A.2, A.4, B.1 and B.2 and are detailed in Fig. 11. Such diagrams admit that apparent pressures should not be less than the ones from the diagram of Terzaghi and Peck. They consider Terzaghi and Peck's value at the ground level and increase linearly down to a depth of 0.4*H*, after which a constant dia-

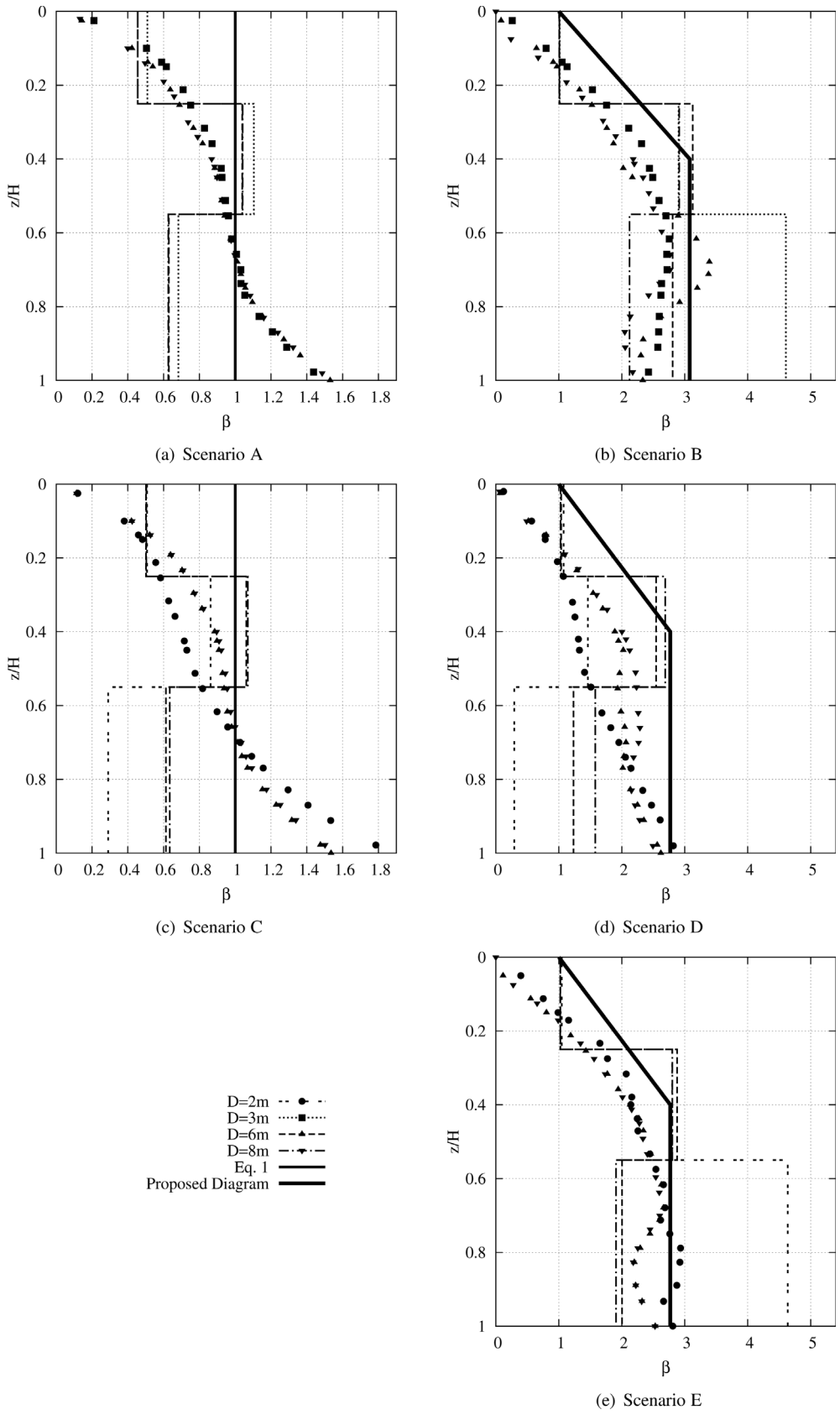

Figure 9 - Analysis of the variation of the embedded length of the wall: Dimensionless pressures on the flexible retaining wall after the last excavation stage (symbols) and apparent pressures inferred from the maximum loads on the struts (lines). Note the difference between the horizontal scales of the graphics on the left and on the right.

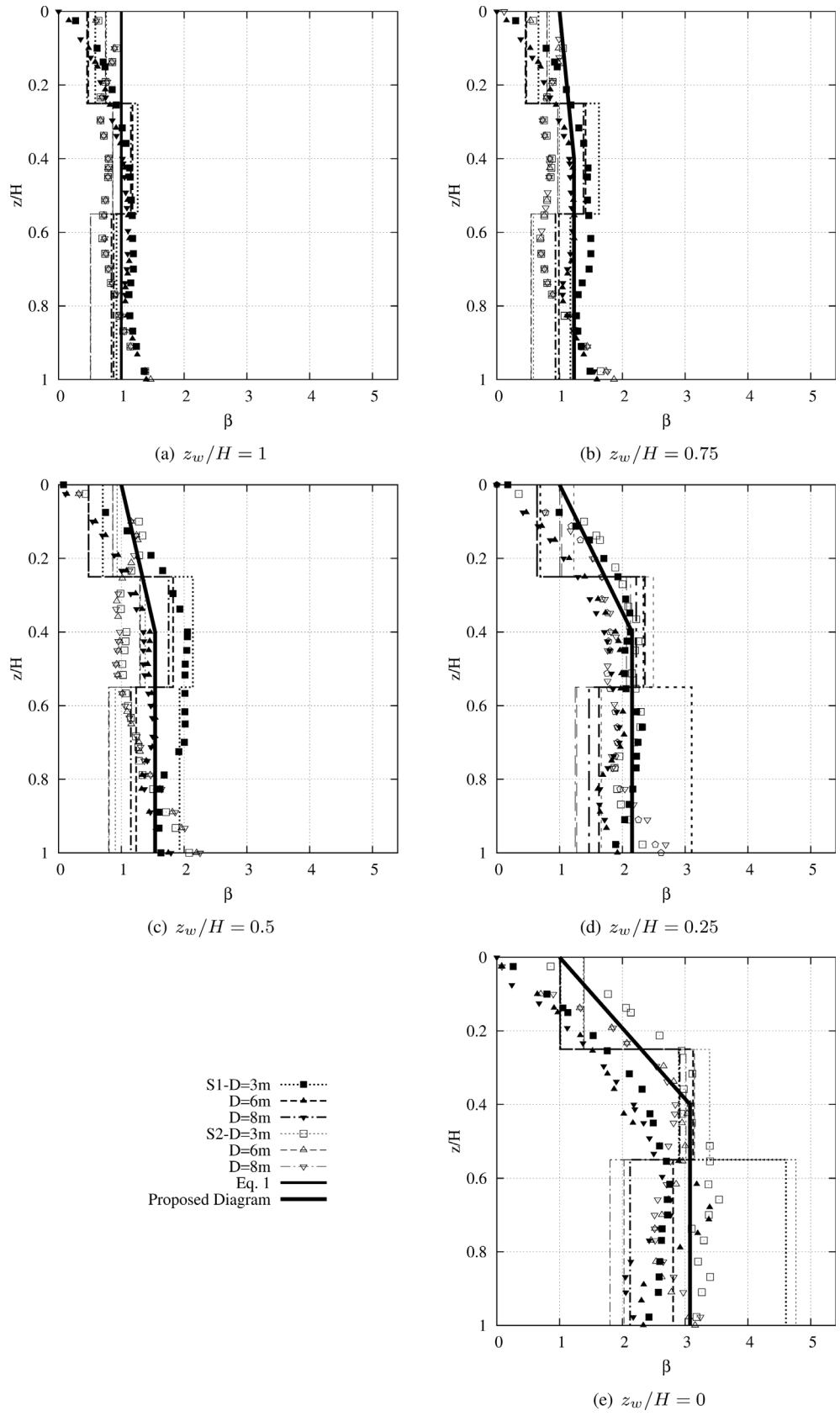

Figure 10 - Scenario B - analysis of the variation of the embedded length of the wall to different depths of the water table: dimensionless pressures on the flexible retaining wall after the last excavation stage (symbols) and apparent pressures inferred from the maximum loads on the struts (lines).

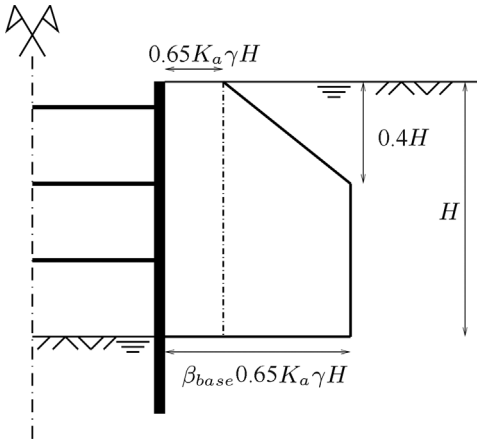

Figure 11 - Proposal for apparent design diagrams.

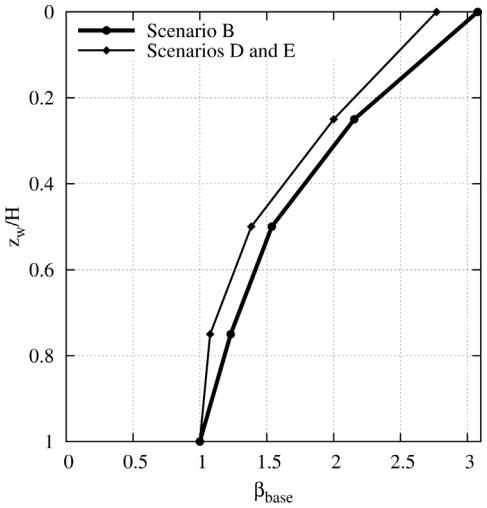

Figure 12 - Proposed values of β_{base} as a function of the depth of the water table.

gram given by a horizontal pressure of β_{base} 0.65 $K_a\gamma H$ is proposed.

In the particular case of water table on the ground surface, it appears from Figs. 9, A.2 and A.4 that the results of the dimensionless pressures can be approximated by β_{base} = 3.1 for scenario B and 2.75 for scenarios D and E. These values show a considerable influence of the water table on total pressures and on the loads on the struts. It should be noted that in the course of the parametric analysis performed, a few cases of very large apparent pressures corresponding to the last strut level were obtained. These few cases mainly correspond to situations where hydraulic uplift safety factors are very low and beyond the scope of usual design. Such cases involve the same type of phenomena also present in undrained situations with poor basal stability conditions (Terzaghi & Peck, 1967; Bjerrum *et al.*, 1972; Peck *et al.*, 1974). Therefore, these situations were ignored for the proposal of the apparent pressure distribution diagrams presented.

Based on the parametric analysis of the variation of the depth of the water table that was performed for scenarios B, D and E (Figs. 10, B.1 and B.2) a chart with the corresponding values of β_{base} (Fig. 12) for different values of z_w is further proposed. The resulting diagrams are shown in Figs. 10, B.1 and B.2.

6. Conclusions

From the developed study it can be concluded that the existing proposals in the literature for the apparent diagrams corresponding to situations in which the water level is considered and seepage is allowed, as well as the situations in which the water level is considered with hydrostatic pressures, are not suitable approximations for the distribution of pressures on the wall or the apparent pressures. Indeed, in all calculations the results achieved were greater than the values corresponding to these diagrams.

The calculations were performed for a relatively wide range of situations, assuming homogeneous and isotropic behaviour of the soil, for two soil conditions, for different geometries (embedded length of the wall, width of the excavation, scale of the problem), different soil unit weights and different stiffnesses of the wall and of the struts. Also, several positions of the water table was considered.

The obtained pressures were normalized using the stress of Terzaghi and Peck's apparent diagram for sands and the normalized results could be reasonably represented by a proposed apparent design diagram for cases in which the water level is assumed, either when seepage is allowed and when hydrostatic pressures are considered. The exceptions correspond to cases with low hydraulic uplift safety factors. The proposed apparent design diagram shows a very large influence of the water table on the pressures on the wall, increasing them significantly.

References

Andrade Viana, L. (2014). Pressões Sobre Cortinas de Contenção em Solos com Nível Freático Elevado. Master's Thesis, UNL, Faculdade de Ciências e Tecnologia, Universidade Nova de Lisboa, Lisboa.

Bjerrum, L., Frimann Clausen, C. & Duncan, J. (1972). Earth pressure on flexible structures - A state of the art report. In: Proc. 5th European Conference on Soil Mechanics and Foundation Engineering, Madrid, volume 2, p. 169-196.

Ebeling, R.M. & Morrison, E.E. (1992). The seismic design of waterfront retaining structures. Technical Report ITL-92-11, U.S. Army Engineer Waterways Experiment Station.

Kaiser, P.K. & Hewitt, K.J. (1982). The efect of groundwater flow on the stability and design of retained excavations. Canadian Geotechnical Journal, 19:139-153.

Peck, R.B., Hanson, W.E. & Thornburn, T.H. (1974). Foundation Engineering. John Wiley and Sons, New York, 2nd edition.

Plaxis (2014). Plaxis 2D Manual. Brinkgreve *et al.*, eds. Delft.

Schanz, T., Vermeer, P.A. & Bonnier, P.G. (1999). The hardening-soil model: Formulation and verification. In: Proc. Beyond 2000 in Computational Geotechnics, Balkema, Rotterdam, p. 281-290.

Strom, R.M. & Ebeling, R.M. (2001). State of the practice in the design of tall, stiff, and flexible tieback retaining walls. Technical Report ITL TR-01-1, US Army Corps of Engineers. Engineer Research and Development Center.

Terzaghi, K. & Peck, R.B. (1967). Soil Mechanics in Engineering Practice. John Wiley & Sons, Inc., 2nd edition.

Appendix A

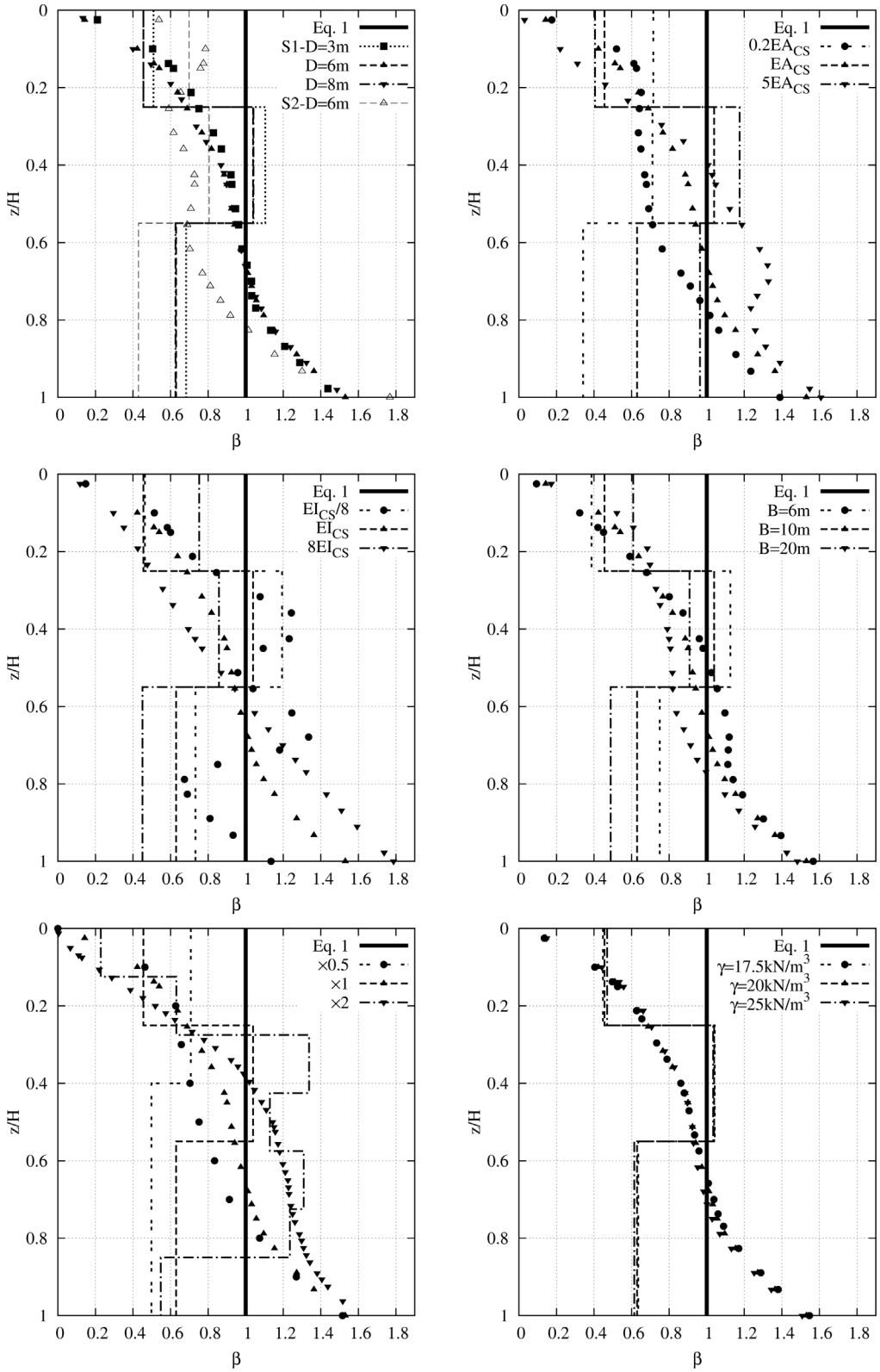

Figure A.1 - Scenario A - analysis of the variation of the: embedded length of the wall; stiffness of the struts; stiffness of the wall; width of excavation; scale and unit weight of the soil. Dimensionless pressures: total stresses on the flexible retaining wall after the last excavation stage (symbols) and apparent pressures inferred from the maximum loads on the struts (lines).

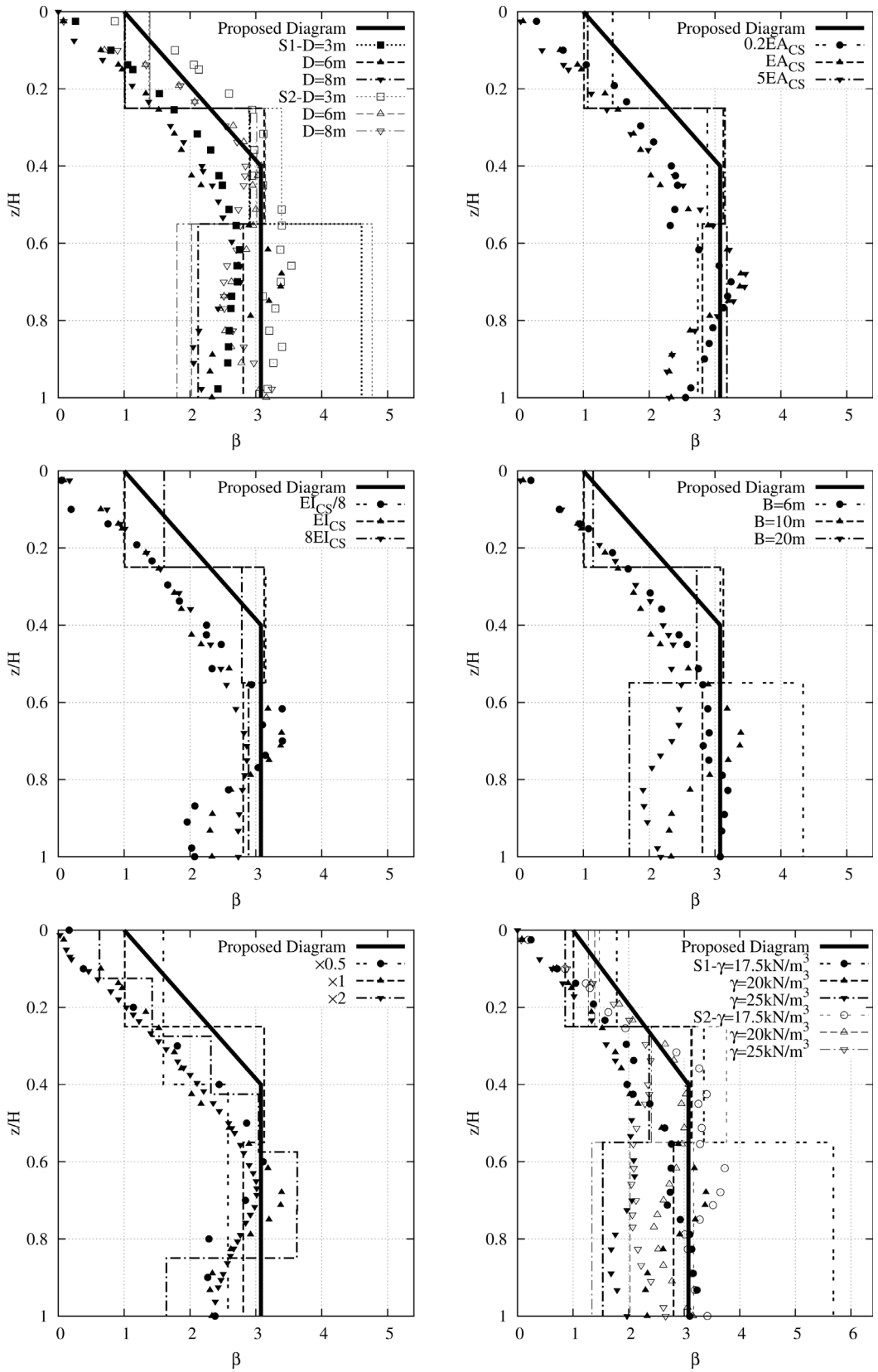

Figure A.2 - Scenario B - analysis of the variation of the: embedded length of the wall; stiffness of the struts; stiffness of the wall; width of excavation; scale and unit weight of the soil. Dimensionless pressures: total stresses on the flexible retaining wall after the last excavation stage (symbols) and apparent pressures inferred from the maximum loads on the struts (lines). Note the difference in the horizontal scale in the bottom right graphic.

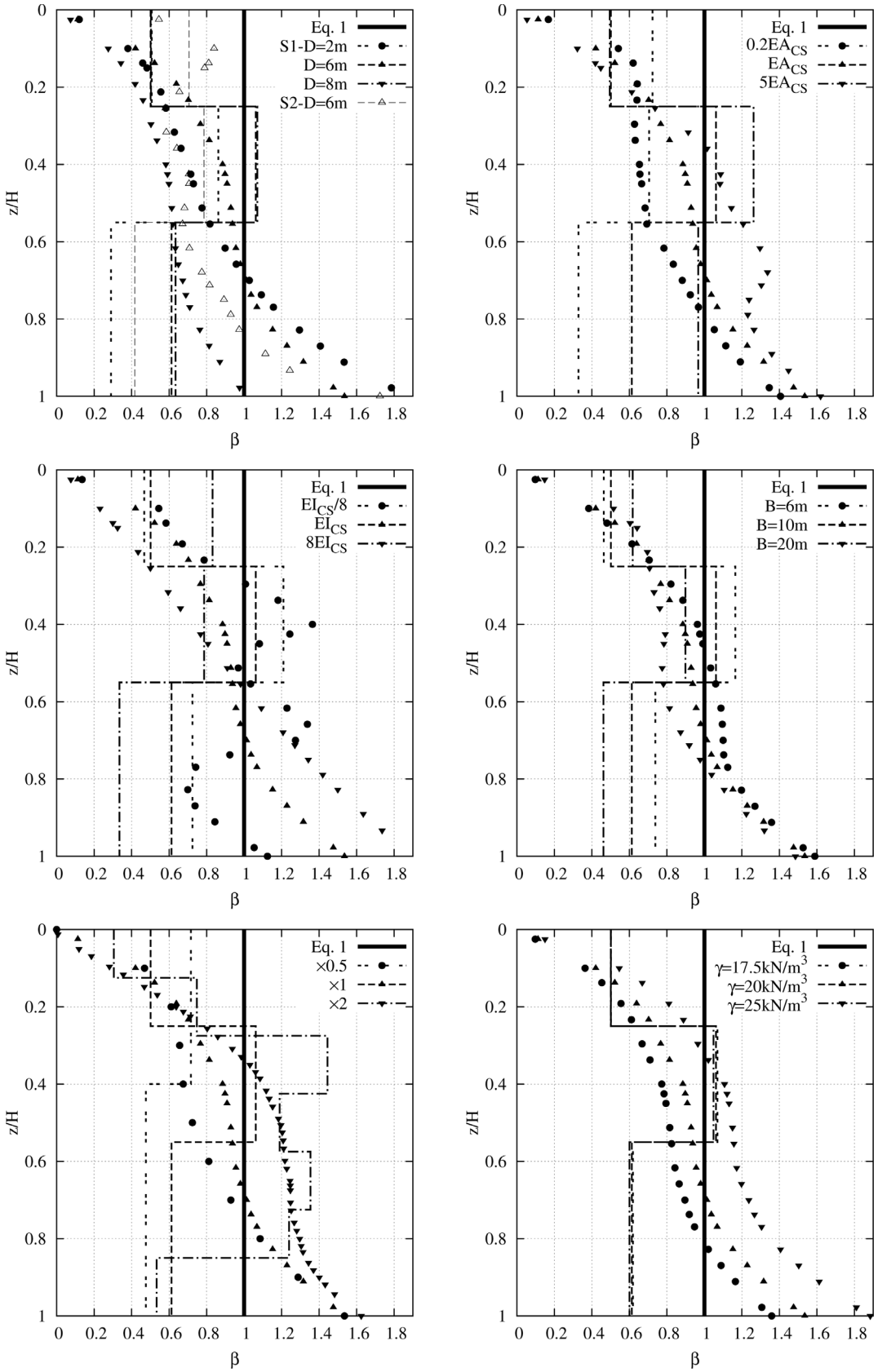

Figure A.3 - Scenario C - analysis of the variation of the: embedded length of the wall; stiffness of the struts; stiffness of the wall; width of excavation; scale and unit weight of the soil. Dimensionless pressures: total stresses on the flexible retaining wall after the last excavation stage (symbols) and apparent pressures inferred from the maximum loads on the struts (lines).

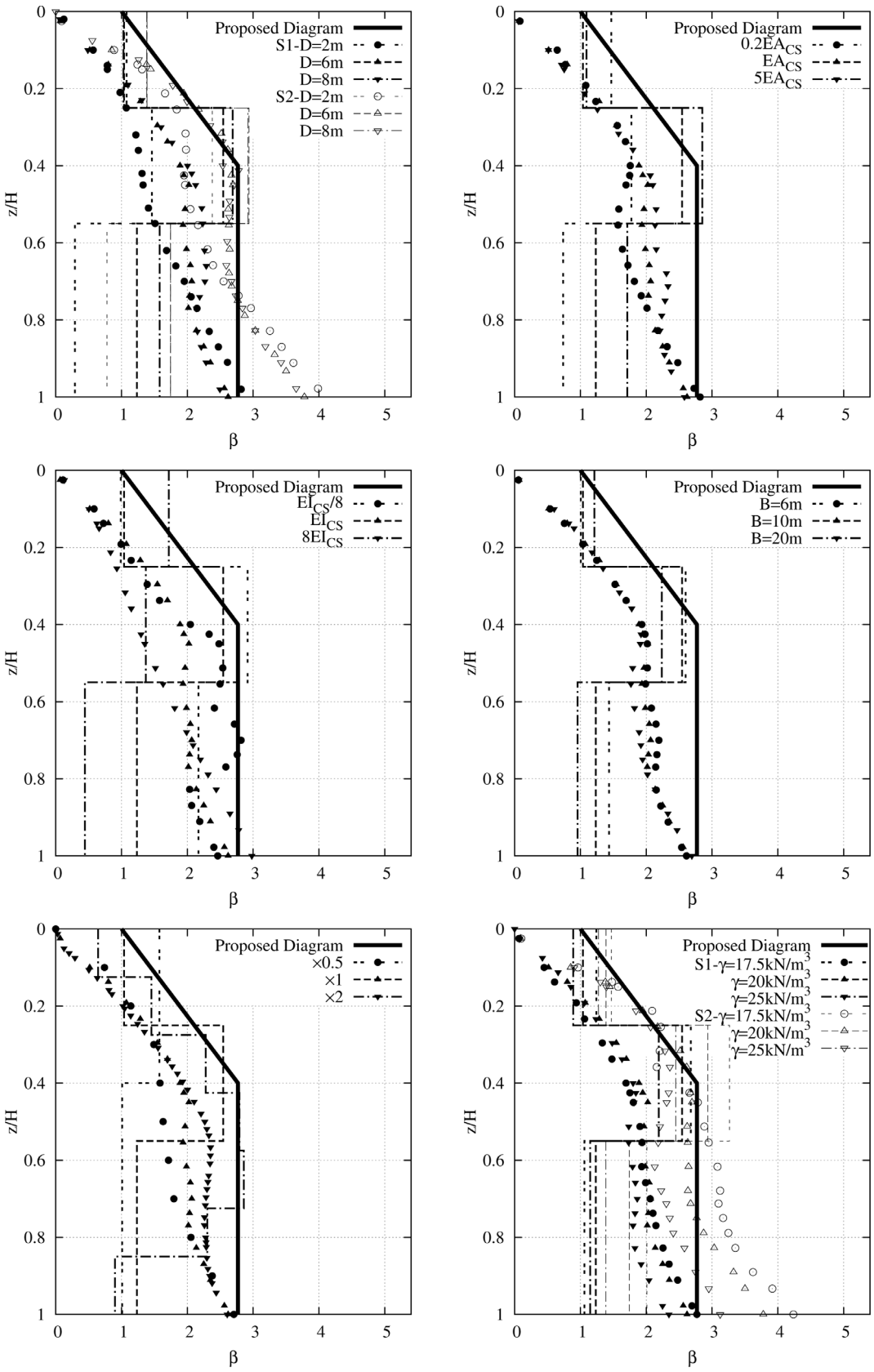

Figure A.4 - Scenario D - analysis of the variation of the: embedded length of the wall; stiffness of the struts; stiffness of the wall; width of excavation; scale and unit weight of the soil. Dimensionless pressures: total stresses on the flexible retaining wall after the last excavation stage (symbols) and apparent pressures inferred from the maximum loads on the struts (lines).

Appendix B

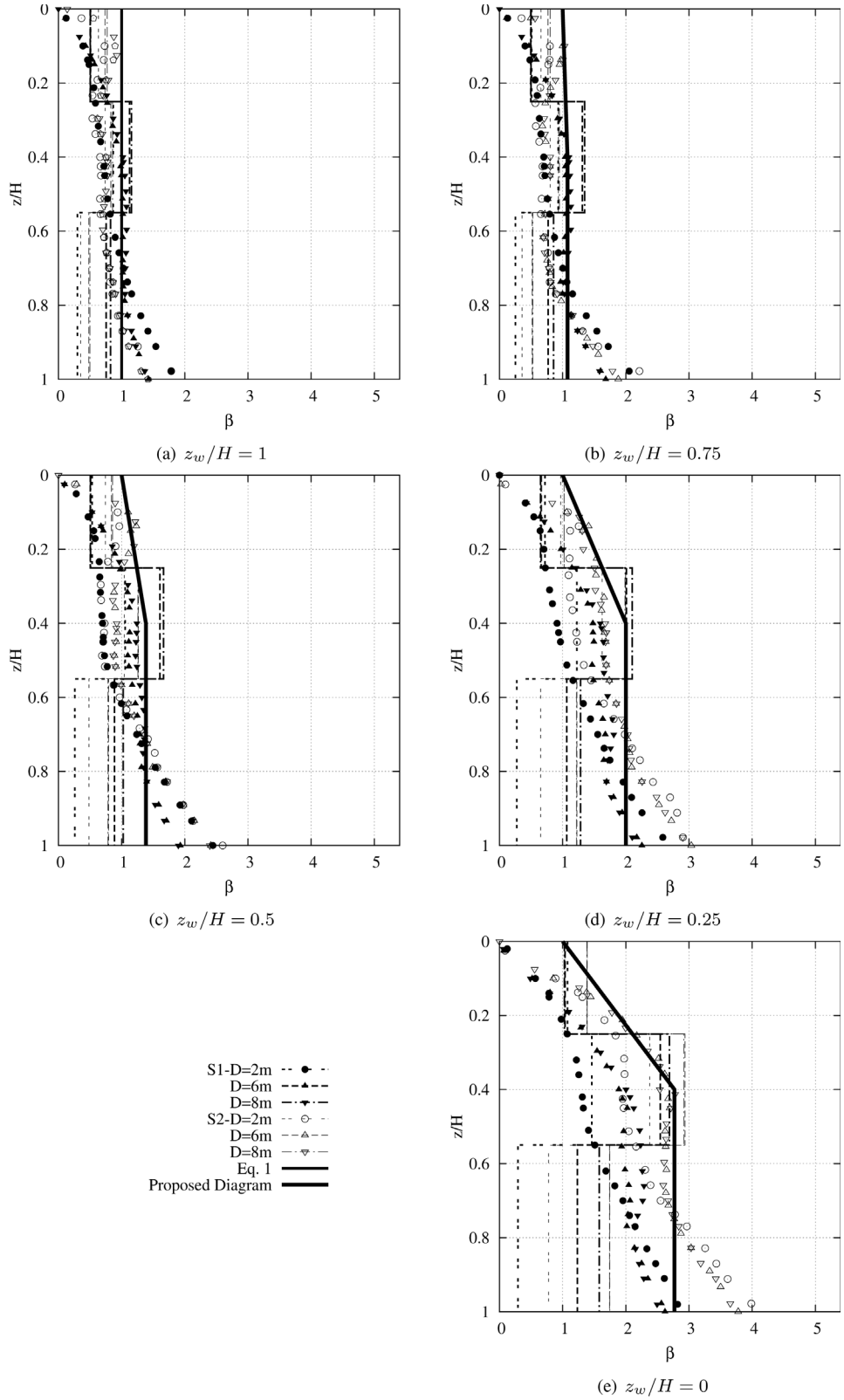

Figure B.1 - Scenario D - analysis of the variation of the embedded length of the wall to different depths of the water table. Dimensionless pressures: pressures on the flexible retaining wall after the last excavation stage (symbols) and apparent pressures inferred from the maximum loads on the struts (lines).

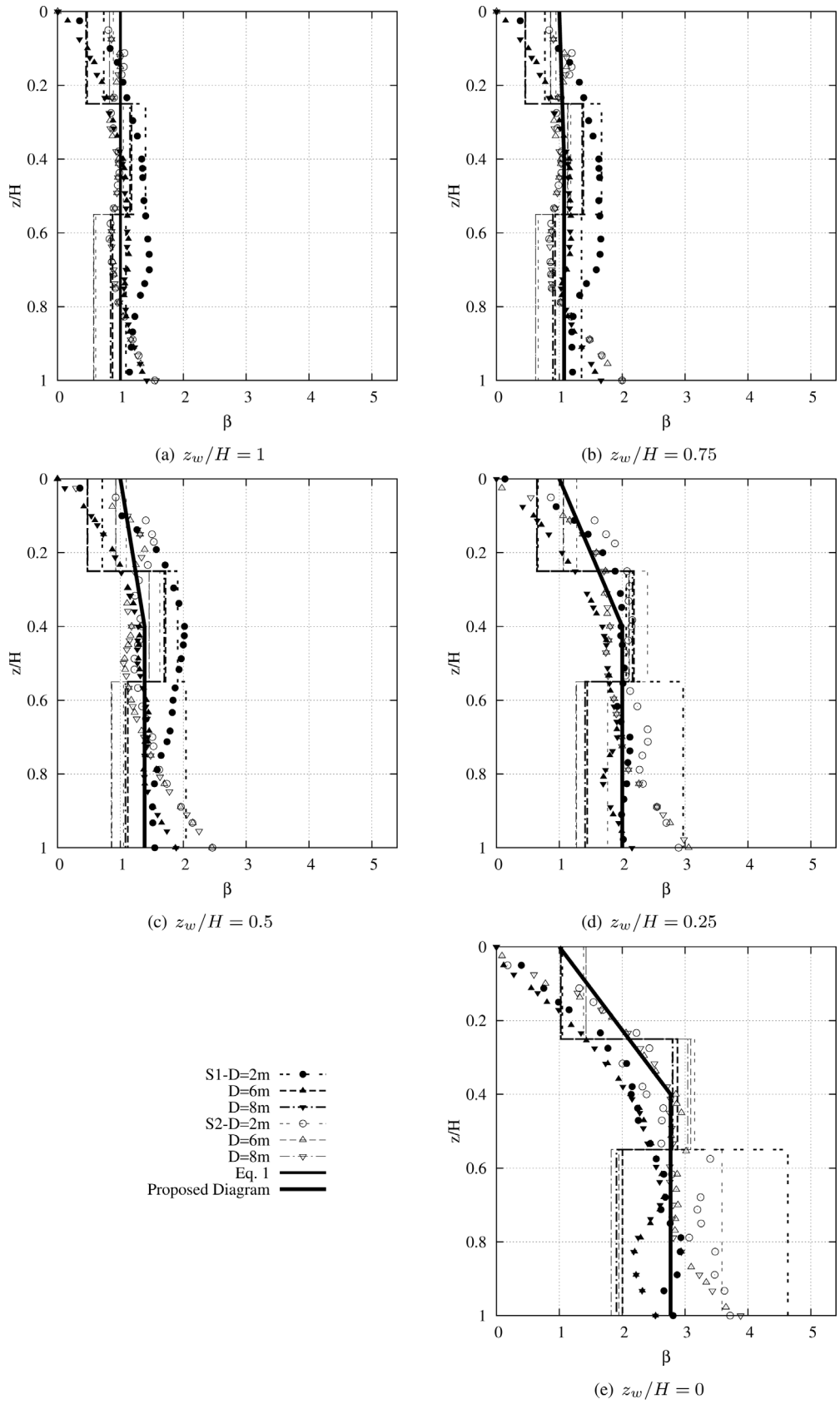

(a) $z_w/H = 1$ (b) $z_w/H = 0.75$

(c) $z_w/H = 0.5$ (d) $z_w/H = 0.25$

(e) $z_w/H = 0$

Figure B.2 - Scenario E - analysis of the variation of the embedded length of the wall to different depths of the water table. Dimensionless pressures: pressures on the flexible retaining wall after the last excavation stage (symbols) and apparent pressures inferred from the maximum loads on the struts (lines).